DEVELOPING THE SIMULATOR FOR PLANETARY INTERACTIONS OF DUST AND REGOLITH (SPIDR). H. M. Sargeant[1,2], J. Long-Fox[1], J. Dyson[2], K. L. Donaldson Hanna[1], and D. Britt[1]. [1]The University of Central Florida (HannahMarie.Sargeant@ucf.edu), [2]The University of Leicester.

Introduction: Simulating lunar dust clouds will be beneficial in addressing dust mitigation efforts by computationally testing alternative rover wheel and fender designs, and different operational modes. The *Simulator for Planetary Interactions of Dust and Regolith* (SPIDR) is a Discrete Element Method (DEM) tool that can be used to model dust (< 50 micron [1]) cloud production. SPIDR simulates the lunar surface environment using LIGGGHTS [2], an open source DEM particle simulation software. Other DEM simulations of planetary regolith focus on bulk properties that mimic the geotechnical behavior of regolith when interacting with hardware such as rovers and excavators [e.g., 3,4]. SPIDR instead is focused on replicating the trajectories of the finest regolith particles that are kicked up from planetary surfaces during rover locomotion, and therefore requires a different approach to modeling individual particles. The geotechnical behavior of particles in SPIDR is only relevant in determining their 'stickiness' to each other and objects such as wheels. Here we describe the SPIDR modelling approach in more detail, and some of the calibration efforts to determine how cohesive lunar particles are.

The SPIDR Approach: With SPIDR, the particle masses are more accurately modelled so that they follow the expected trajectories of dust particles on the Moon. The vast majority of lunar regolith materials have a particle size <50 μm, and the smallest particles are most susceptible to lofting and forming dust clouds. Therefore, we will only be modelling particle sizes in this region ($\bar{r}$=1.5-13.3 μm). We analyzed the average lunar particle size distribution reported in wt.% fractions [1], and calculated the particle mass of these fractions when assuming an average grain density of 3365 kg m^{-3} [5]. The four particle size bins in this region represent the four particle sizes we have included in the simulation, and they are reported in Table 1. A difference in particle size of a factor of ≤ 10 is optimal when using LIGGGHTS as the skin depth (the region in which particle-particle interactions occur) is of the same magnitude.

Table 1 SPIDR particle size distribution (pre scaling)

Particle size, $\bar{r}$ (μm)	Particle mass (kg), $\bar{m}$	Ratio of total number of particles (%), R_{number}
13.3	1.22×10^{-10}	1
7.4	3.33×10^{-11}	3
3.7	5.80×10^{-12}	26
1.5	7.25×10^{-13}	70

To accommodate the scale of the expected modelling setups, we have increased the particle radius size in SPIDR by a factor of 50. The density of the particles was scaled accordingly so that the particles still have the same mass. This will result in a different bulk regolith behavior to those shown in the other DEM models found in the literature [2,3] as the bulk mass is significantly reduced.

Calibrating cohesion and friction: The remaining particle properties to be defined are the cohesion and friction values which dictate how the particles move across each other and other surfaces (such as wheels). For example, as a wheel moves through the particles, some particles will adhere to the wheel and other particles. The cohesion and friction values affect the critical amount of force needed to separate particles and cause them to be released into a dust cloud.

The different cohesive mechanisms found in lunar regolith can be simplified in the DEM to an idealized term to approximate the cohesive properties and minimize computational effort [6]. We utilized the modified Simplified Johnson-Kendall-Roberts (SJKR2) model in LIGGGHTS that considers a single cohesive parameter, the Cohesion Energy Density, *CED* (Jm^{-3}). With the SJKR2 model, bulk material flow behavior is dependent on the coefficient of particle-on-particle friction, μ_p, the coefficient of rolling friction, μ_r, and *CED*. These parameters can be derived experimentally using a simple calibration 'lifting cylinder' slope failure test [6]. In the lifting cylinder test, a cohesive material is poured into a hollow cylinder, and the cylinder is then raised up such that the only forces acting on the bulk material column are gravity and those of the material itself (Figure 1). The column deformation and flow behavior can be recorded and compared to simulations performed with SPIDR, which replicates the experiment. The SPIDR simulations were repeated for a range of μ_p, μ_r, and *CED* values.

Experimental Results: We performed the lifting cylinder test on two Apollo bulk regolith samples, a mare sample (15071) and a highlands sample (61141) [7]. The test is independent of cylinder size, and therefore we opted for a smaller cylinder size (h=25.2 mm, ID=8.52 mm) than that used in the experiments of [6] as we had access to a limited sample size of ~2 g for each of the Apollo regolith samples. The funnel was lifted with a constant velocity of 8.7±0.2 mm s^{-1}. Each experiment was repeated three times and a camera was used to record the deformation and flow of the granular

material from the cylinder with a frame rate of 30 fps. The video footage was analyzed, and column width was measured as the cylinder base reached the selected heights, *h*. The SPIDR simulation results were analyzed with a Python script which measured the same column width values as in the analysis of the experimental results. The script then identified the resultant simulation that exhibited the most similar (lowest error) column width deformation at each stage of the experiment. The best-fit parameter values are those used in the optimized simulation.

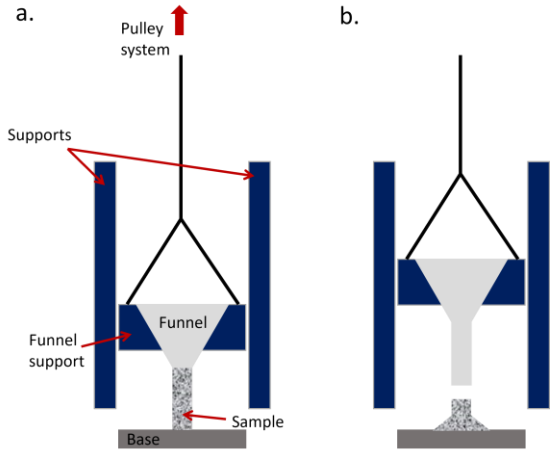

Figure 1. Lifting cylinder test experimental setup.

Results of each lifting cylinder test for each sample type were highly variable, as the point of column collapse occurred at different *h* values. It is assumed that small vibrations during the cylinder lifting process could have caused early column collapse. Therefore, we selected the results exhibiting the most cohesion (least column deformation) to compare our simulations to. The best-matched SPIDR simulation is shown in Figure 2 alongside the results of the 15071 experiment. It can be seen that there is some visible equivalence to the two sets of results, with initial column stability and final pile dimensions. However, the stage at which column deformation occurs is not the same.

Limitations and next steps: The highlands samples exhibited slightly more cohesive behavior with later column collapse and higher angles of repose compared to the mare samples. However, while scanning through the different cohesion and friction variables with the SPIDR calibration simulations, the same combination of variables (μ_p=0.5, μ_r=0.5, and *CED*=6) was shown to best match both the highlands and mare samples. This suggests that the chosen variable range did not include sufficient resolution to identify the differences described. We suggest a second calibration campaign to identify the optimal variables that represent the different terrain types. The variables identified here will be used in SPIDR for generic lunar regolith.

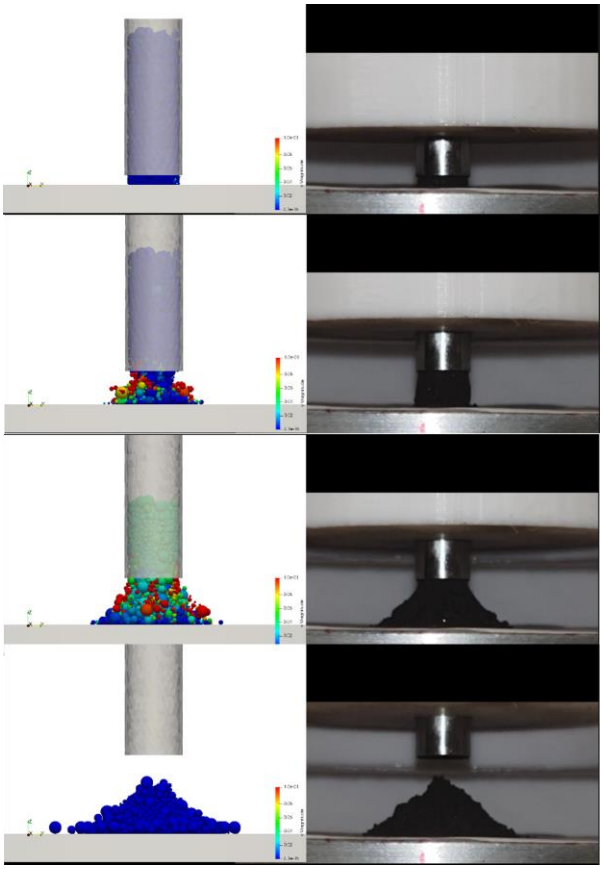

Figure 2. Lifting cylinder results. Left – optimized LIGGGHTS simulation, Right – sample 15071.

The lifting cylinder test is supposedly scale-independent. However, initial testing with the SPIDR simulations suggest that when simulating larger cylinders, the column deformation behavior changes. We suggest a lower limit on the geometry-to-particle-size ratio that would result in different bulk behavior. We will therefore need to repeat the calibration campaign with larger cylinder geometries.

Acknowledgements: This work was funded by the European Commission through its Horizon 2020 Programme Grant Agreement #822018 and by CLASS NASA Cooperative Agreement #80NSSC19M0214. We are grateful to the TIRES-LSCC for loaning the samples used in this study

References: [1] Zeng X. et al. (2010) *Jour. of Aero. Eng.*, 23(4), pp. 213-218. [2] CFDEM Project (2021) *LIGGGHTS*, https://www.cfdem.com/liggghtsr-open-source-discrete-element-method-particle-simulation-code. [3] Zhu J. et al. (2022) *Act. Astro.*, 191, pp. 169-177. [4] Jiang M. et al. (2017) *Jour. of Terramech.*, 71, pp. 1-13. [5] Kiefer W. et al. (2012) *Geophys. Res. Let.*, 39(7) pp.1-5. [6] Roessler & Katterfeld (2019) *Particuology*, 45, pp. 105-115. [7] Donaldson Hanna K. L. et al. (2017) *Icarus*, 283, pp. 326-342.